

Theme II: Studies on damping and energy absorption of structures

Objekttyp: **Group**

Zeitschrift: **IABSE reports of the working commissions = Rapports des commissions de travail AIPC = IVBH Berichte der Arbeitskommissionen**

Band (Jahr): **13 (1973)**

PDF erstellt am: **11.09.2024**

Nutzungsbedingungen

Die ETH-Bibliothek ist Anbieterin der digitalisierten Zeitschriften. Sie besitzt keine Urheberrechte an den Inhalten der Zeitschriften. Die Rechte liegen in der Regel bei den Herausgebern.

Die auf der Plattform e-periodica veröffentlichten Dokumente stehen für nicht-kommerzielle Zwecke in Lehre und Forschung sowie für die private Nutzung frei zur Verfügung. Einzelne Dateien oder Ausdrucke aus diesem Angebot können zusammen mit diesen Nutzungsbedingungen und den korrekten Herkunftsbezeichnungen weitergegeben werden.

Das Veröffentlichen von Bildern in Print- und Online-Publikationen ist nur mit vorheriger Genehmigung der Rechteinhaber erlaubt. Die systematische Speicherung von Teilen des elektronischen Angebots auf anderen Servern bedarf ebenfalls des schriftlichen Einverständnisses der Rechteinhaber.

Haftungsausschluss

Alle Angaben erfolgen ohne Gewähr für Vollständigkeit oder Richtigkeit. Es wird keine Haftung übernommen für Schäden durch die Verwendung von Informationen aus diesem Online-Angebot oder durch das Fehlen von Informationen. Dies gilt auch für Inhalte Dritter, die über dieses Angebot zugänglich sind.

Valeurs et représentation de la capacité d'amortissement

Werte und Darstellung der Dämpfungsfähigkeit

Values and Representation of Damping Capacity

P. MAZILU

Professeur de résistance des matériaux
Institut des Constructions
Bucarest, Roumanie

H. SANDI

Chef du laboratoire de mécanique des structures
Institut de Recherches du Bâtiment (INCERC)
Bucarest, Roumanie

1. Quelques déterminations de la capacité d'amortissement des vibrations

Il est un fait bien connu, issu des résultats obtenus à la suite de nombreuses recherches, que la capacité d'amortissement des vibrations est fortement variable d'un cas à l'autre. Le type de structure et les liaisons avec les corps environnants, aussi bien que l'état de sollicitation, ont une influence sensible, même spectaculaire, sur la capacité des structures d'absorber de l'énergie de vibration. Quoique la littérature de spécialité présente une grande quantité de données à ce sujet, on juge comme utile de résumer dans le tableau 1 quelques résultats obtenus pendant les dernières années par les chercheurs roumains, à la suite de l'utilisation de différents techniques expérimentales.

Tableau 1

No	Type de structure	Technique d'essai	Méthode d'analyse	Valeurs de "n"	Référence	Commentaire
1.	Barrages-voûte, encastrés dans des massifs rocheux	Explosions souter- raines de faible intensité	Mesurement du décrément logarithmique	0,004 à 0,008	[7]	Valeurs spécifiques pour le comportement linéaire
2.	Bâtiments résidentiels ou administratifs à 8 ...25 étages	Agitation microsismique permanente	Examination qualitative des vibrogrammes	Pas de valeurs précises	[8]	Discussion à la suite du tableau
3.	Structures industrielles soumises à l'action des ponts-roulants	Fonctionnement des ponts-roulants	Analyse du décrément logarithmique	0,015 à 0,025 (métal) 0,02 à 0,04 (béton armé)	INCERC, Bugheanu	Des différences sensibles entre les structures et même entre les modes de vibration

4.	Structure en béton armé à microsis-cadres, avec antenne en acier	Agitation micro-sismique	Examina-tion quali-tative des vibro-grammes	Pas de valeurs précises	INCERC, Şerbănescu, Zorapapel	Discussion à la suite du tableau
5.	Eléments préfabriqués cylindriques en béton pré contraint, pour les toitures	Chocs de faible intensité	Mesurement du décrément logarithmique	0,003	[1]	Superposi-tion des mou-vements de flexion et de torsion
6.	Fragments de grands panneaux à joints par boucles bétonnées	Chocs de forte intensité	Mesurement du décrément logarithmique	0,04 à 0,06 av. fissuration 0,07 à 0,11 avec fissures partielles 0,11 à 0,18 après fissuration complète	IEB, Mazilu	Influence décisive du développe-ment des fissures dans les joints
7.	Modèles de structures en grands panneaux, à différents systèmes de joints, à l'échelle 1: 4	Générateurs de vibrations. Essais jusqu'à la rupture	Analyse de la courbe de réso-nance	0,03 à 0,09, avec forte in-fluence du système de joints et de l'état de solli-citation	[9], INCERC, Şerbănescu, Zorapapel	Tendance de stabilisati-on des va-leurs pour les hauts niveaux de sollicitati-on
8.	Modèles de diaphragmes en béton armé, à l'échelle 1:4	Flexion dy-namique, à l'aide des générateurs de vibrations	Analyse de la courbe de réso-nance	0,04 à 0,14	[3]	Tendance de stabilisati-on à des va-leurs de l'ordre 0,04 à 0,07

L'utilisation de l'agitation micro-sismique comme agent perturbateur ne permet pas d'obtenir des conclusions fermes sur la capacité d'amortissement lorsque l'on ne dispose pas de la possibilité d'effectuer une analyse automatique, correlative ou spectrale, des enregistrements obtenus. Néanmoins, l'observation visuelle des vibrogrammes est hautement instructive. Elle permet de comparer les sélectivités des différentes structures et même de remarquer une différence qualitative du comportement des différentes parties des structures. Par exemple, les essais mentionnés au No. 2 du tableau ont permis de mettre en évidence de hautes sélectivités de quelques structures (dus surtout à des conditions particulières de fondation). Tout de même, l'essai mentionné au No. 4 du tableau a permis d'observer un comportement tout spécial: oscillation de l'infrastructure en béton armé avec une fréquence prédominante de l'ordre de 1 Hz., tandis que la tour en acier oscillait presque sinusoïdalement, avec une fréquence de 3,2 Hz. (les problèmes analysés au paragraphe 4 de la discussion sont d'intérêt direct pour ce dernier cas).

2. Localisation de la capacité d'amortissement

La capacité d'amortissement peut être analysée dans le stade de comportement linéaire des matériaux à l'aide des relations établies pour une vibration sinusoïdale. Si les différents paramètres des vibrations peuvent être exprimés sous la forme

$$f(t) = \text{Re} [\hat{f}(i\omega) e^{i\omega t}] \quad (1)$$

il existe, pour chaque fréquence circulaire ω , une relation entre les amplitudes complexes des tensions et des déformations, de la sorte

$$\hat{s}(i\omega) = \hat{B}(i\omega) \hat{e}(i\omega) \quad (2)$$

Si l'on peut établir une relation analytique (2), valable pour un ensemble de valeurs ω ayant au moins un point d'accumulation à distance finie, cette relation peut être prolongée analytiquement dans le plan complexe

$$p = \chi + i\omega \quad (3)$$

et peut être considérée comme l'image Laplace-Carson d'une loi rhéologique entre les tensions $s(t)$ et les déformations $e(t)$ (la transformation intégrale bilatérale Laplace-Carson entre l'original $f(t)$ et son image $\hat{f}(p)$ a la forme [10])

$$\begin{aligned} \hat{f}(p) &= p \int_{-\infty}^{\infty} e^{-pt} f(t) dt \quad (\text{Re } p \in \text{domaine de convergence}) \\ f(t) &= \frac{1}{2\pi i} \int_{\chi-i\infty}^{\chi+i\infty} \frac{e^{pt}}{p} \hat{f}(p) dp \quad (\text{Re } p = \text{const.}) \end{aligned} \quad (4)$$

où il faut prêter l'attention nécessaire à la valeur $\text{Re } p$, qui détermine le domaine de convergence de la transformation).

En particulier, le modèle rhéologique Kelvin-Voigt correspond à un coefficient

$$\hat{B}(i\omega) = E + i\omega\eta \quad (5)$$

(E : module d'élasticité, η : module de viscosité) ou, bien, pour l'original,

$$B(t) = E H(t) + \eta \frac{d}{dt} \quad (H(t): \text{fonction de Heaviside}) \quad (6)$$

La quantité $\text{Re} [\hat{B}(p)]$ doit être strictement positive pour toute l'axe imaginaire $p = i\omega$ (corps solide), tandis que la quantité $\text{Im} [\hat{B}(i\omega)]$ doit être non-négative pour toute l'axe, lorsqu'il n'existe pas de source d'énergie interne. De plus, $\text{Re} [\hat{B}(p)] = \text{Re} [\hat{B}(\bar{p})]$ et $\text{Im} [\hat{B}(p)] = -\text{Im} [\hat{B}(\bar{p})]$ (\bar{p} : conjugué complexe de p) lorsque la loi rhéologique pour l'original ne contient pas de termes complexes. Les zéros de la fonction $\hat{B}(p)$ sont des points du spectre de fluage du matériau (variation d' $e(t)$ pour $s(t)$ constant), tandis que les poles de cette fonction sont des points du spectre de relaxation du matériau (variation de $s(t)$ pour $e(t)$ constant). Pour un modèle Kelvin la condition $\hat{B}(p) = 0$ conduit à la valeur

$$p_{fl} = -\frac{E}{\eta} \quad (7)$$

et donc, à des phénomènes de fluage du type

$$e(t) = e_0 e^{p_{fl} t} = e_0 e^{-\frac{Et}{\eta}} = e_0 e^{-\frac{t}{T_{ret}}} \quad (T_{ret} = \frac{1}{p_{fl}}) \quad (8)$$

Si, pour un processus de déformation caractérisé par une relation (2), l'on compare l'énergie spécifique de déformation maximum par cycle, E_1 , et l'énergie dissipée par cycle, E_2 ,

$$E_1 = \frac{1}{2} |\hat{s}(i\omega)| \cdot |\hat{e}(i\omega)| \cos \arg \hat{B}(i\omega) \quad (9)$$

$$E_2 = \pi |\hat{s}(i\omega)| \cdot |\hat{e}(i\omega)| \sin \arg \hat{B}(i\omega)$$

le rapport ψ , donné par la relation

$$\Psi = \frac{E_2}{E_1} = 2\pi \frac{\text{Im} [\hat{B}(i\omega)]}{\text{Re} [\hat{B}(i\omega)]} \quad (10)$$

est une mesure de la capacité d'amortissement qui permet une analyse approfondie du mécanisme d'absorption de l'énergie. Les différences de phase entre les tensions et les déformations, déterminées par le rapport $\text{Im} [\hat{B}(i\omega)] / \text{Re} [\hat{B}(i\omega)]$ permettent d'analyser la localisation des pertes d'énergie, donc de la capacité d'amortissement.

Le problème de définir un coefficient Ψ pour un corps non-homogène est délicat, puisque l'on peut sommer d'une manière naturelle les quantités E_2 , mais pas les quantités E_1 , lorsqu'il s'agit de différences de phase entre les différentes parties d'un corps.

3. Modèles rhéologiques linéaires élémentaires

Le modèle rhéologique linéaire le plus simple de matériau solide non-élastique est le modèle Kelvin, donné par la relation (6) ou par sa transformée Laplace-Carson,

$$\hat{B}(p) = E + \eta p \quad (11)$$

Ce modèle a un point du spectre de fluage, donné par la relation (9). Le modèle, largement utilisé dans la dynamique des structures, présente l'inconvénient majeur de conduire à une capacité d'amortissement proportionnelle à la fréquence circulaire:

$$\frac{\Psi}{2\pi} = \frac{\text{Im} [\hat{B}(i\omega)]}{\text{Re} [\hat{B}(i\omega)]} = \frac{\eta \omega}{E} \quad (12)$$

qui est en contradiction directe avec l'expérience.

Le modèle de complexité suivante est celui de Poynting,

$$\hat{B}(p) = E_0 + \frac{p \eta_1}{1 + \frac{p \eta_1}{E_1}} \quad \left(\begin{array}{l} E_0 = E_{\text{statique}}, \\ E_1 = E_{\text{dynamique}} - E_0 \end{array} \right) \quad (13)$$

qui a un point du spectre de fluage, $p_{fl.}$, et un point du spectre de relaxation, $p_{rel.}$, donnés par les relations

$$p_{fl.} = - \frac{E_0}{(1 + \frac{E_0}{E_1}) \eta_1} \quad (T_{ret} = 1/p_{fl.})$$

$$p_{rel.} = - \frac{E_1}{\eta_1} \quad (T_{rel} = 1/p_{rel.}) \quad (14)$$

Ce modèle, plus perfectionné que le précédent, a toutefois l'inconvénient de conduire à une capacité d'amortissement qui disparaît pour de très hautes fréquences.

Le modèle de Poynting peut être encore corrigé par le modèle de Maxwell généralisé,

$$\hat{B}(p) = E_0 + \sum_i^{1,n} \frac{p \eta_i}{1 + \frac{p \eta_i}{E_i}} \quad (15)$$

qui présente plusieurs points pour les spectres de fluage et de relaxation. Ce modèle permet une approximation des propriétés d'amortissement observées expérimentalement pour une bande de fréquences convenablement large.

Le modèle de l'amortissement constant,

$$\hat{B}(p) = E (1 + i \gamma) \quad (16)$$

est souvent en bonne correspondance avec l'expérience, mais présente les inconvénients de ne pas permettre d'obtenir un original réel ou des phénomènes de fluage et, aussi, de présenter une capacité d'amortissement qui ne disparaît pas pour de très basses fréquences.

En conclusion il semble que, pour une analyse théorique, concernant aussi l'analyse des mouvements vibratoires linéaires des structures, il est convenable de chercher une approximation des propriétés observées par une loi du type (15), dont les coefficients seront déterminés en partant des phénomènes de mouvement sinusoïdal.

4. Formulation des problèmes de la dynamique des structures

Une structure réduite à un système à n degrés de liberté, dont les déplacements sont représentés par un vecteur n -dimensionnel $U(t)$, soumise à un système de forces sinusoïdales, dont les amplitudes complexes constituent le vecteur $\hat{F}(i\omega)$, va effectuer des vibrations linéaires satisfaisant une équation matricielle de la forme

$$[-\omega^2 M + \hat{K}(i\omega)] \cdot \hat{U}(i\omega) = \hat{F}(i\omega) \quad (17)$$

où $\hat{U}(p)$ est l'image du vecteur $U(t)$, M représente la matrice d'inertie, lorsque $\hat{K}(i\omega)$ représente la matrice de rigidité. En cas de l'existence de liaisons internes exclusivement visco-élastiques du type Kelvin, la matrice $\hat{K}(i\omega)$ aura la forme

$$\hat{K}(i\omega) = K_0 + i\omega C_0 \quad (18)$$

(K_0 : matrice de rigidité élastique; C_0 : matrice de rigidité visqueuse).

La matrice $\hat{K}(i\omega)$ est (en cas de l'hypothèse (18), aussi que dans celui d'hypothèses plus générales) symétrique mais complexe, donc non plus auto-adjointe. Les valeurs propres deviendront en ce cas complexes, tel que les vecteurs propres. En cas des valeurs propres multiples, il n'est plus possible, en général, de déterminer une base complète de vecteurs propres, mais il faut faire appel aux vecteurs principaux pour arriver à une base n -dimensionnelle convenable. Une voie utilisée dans la littérature [2], [5] consiste à formuler un problème de valeurs propres $2n$ -dimensionnel. Cette voie, qui est utilisable seulement en partant de l'hypothèse (18), conduit à des valeurs propres qui correspondent aux vibrations propres (atténuées) du système considéré.

Dans le cas d'une matrice $\hat{K}(p)$ plus générale, il est convenable d'adopter un point de vue différent [6]. On associe à l'équation (17) le problème de valeurs propres n -dimensionnel, fonction du paramètre p ,

$$[-\lambda(p) M + \hat{K}(p)] \cdot \hat{U}(p) = 0 \quad (19)$$

Les solutions $\lambda_r(p)$ et $\hat{U}_r(p)$ ($r = 1 \dots n$) permettent d'établir l'expression de la matrice de transfert, $\hat{H}(p)$, pour chaque valeur p ,

$$\hat{H}(p) = \sum_r \frac{\hat{U}_r(p) \hat{U}_r^T(p)}{[\lambda_r(p) + p^2] \cdot M_r} \quad (M_r = \hat{U}_r^T(p) \cdot M \cdot \hat{U}_r(p)) \quad (20)$$

(cette expression doit être généralisée pour des points p' avec des valeurs propres multiples). Lorsque l'on veut déterminer les vibrations propres atténuées, il faut chercher les poles de $\hat{H}(p)$, donnés par la relation

$$\lambda_r(p) + p^2 = 0.$$

Bibliographie

1. Șt. Bălan, M. Arcan
(sous direction de) Essai des Constructions
Eyrolles, 1972
2. T. K. Caughey, M. E. J.
O'Kelly General theory of vibrations of damped
linear dynamic systems.
C.I.T. Report, 1963.
3. D. Dumitrescu, I. Brînzan,
H. Sandi, G. Șerbănescu Modèles de diaphragmes en béton arme, soumis
à de fortes sollicitations dynamiques.
Colloque RILEM, Mexico City, 1966.
4. F. Eirich
(edited by) Rheology, theory and applications.
Academic Press, N.Y., 1956
5. M. E. J. O'Kelly Vibration of viscously damped linear
dynamic systems.
C.I.T. Report, 1964.
6. H. Sandi Eigenwertaufgaben und Übertragungsmatrizen
für nichtkonservative mechanische Systeme.
ZAMM, 5, 1970.
7. H. Sandi, D. Dragomir,
I. Toma Experimental studies on the normal vibration
modes of arch dams.
Colloque RILEM, Bucarest, 1969.
8. H. Sandi, G. Șerbănescu Experimental results on the dynamic defor-
mation of multi-story buildings.
Proc. 4wcee, Santiago, 1969.
9. G. Șerbănescu, H. Sandi,
T. Zorapapel Dynamic model tests of a large-panel
structure.
Colloque RILEM, Bucarest, 1969.
10. B. Van der Pol, H. Bremmer Operational calculus based on the two-sided
Laplace transform.
(transl. into Russian), Moscow, 1952.

RESUME

La contribution présente d'abord quelques résultats sur la capacité d'amortissement obtenus sur des structures grandeur nature ou sur des modèles à grande échelle. On s'occupe ensuite de la localisation de la capacité d'amortissement et on discute l'utilisation des modèles rhéologiques élémentaires linéaires. Finalement on s'occupe de la formulation des équations de mouvement et des problèmes de la dynamique des structures.

ZUSAMMENFASSUNG

Es werden einige quantitative Ergebnisse über die Dämpfungsfähigkeit von Naturmassstabbauwerken und Grossmassstabmodellen angegeben. Die Arbeit befasst sich dann mit der Lokalisation der Dämpfungsfähigkeit und erörtert die Anwendung linearer elementarer rheologischer Modelle. Schliesslich werden die Formulierung der Bewegungsgleichungen und die Aufgaben der Baudynamik betrachtet.

SUMMARY

Some quantitative results on the damping capacity obtained on fullscale structures and on large-scale models are first presented. Localisation of damping capacity is then dealt with. The use of linear elementary rheological models is discussed. Finally the formulation of equations of motion and of problems of dynamics is dealt with.

Some Empirical Facts on Damping of Bridges

Quelques données empiriques sur l'amortissement des ponts

Einige empirische Tatsachen über Dämpfung von Brücken

Manabu ITO
Professor of Civil Engineering
University of Tokyo

Tsuneo KATAYAMA
Associate Professor
Institute of Industrial Science
University of Tokyo
Japan

Tagahiko NAKAZONO
Chief Engineer
Sakurai Iron Works, Co., Tokyo

1. INTRODUCTION

In the dynamic analysis of bridges, the structural damping has been treated as linear within the elastic range of structure. Therefore, the hysteretic damping is scarcely taken into account with bridge structures. Another important feature of the damping of bridge is the difference in its characteristics between superstructures and substructures. The damping values for piers are widely scattered as those for buildings, while those for bridge superstructures fall within a relatively narrow range of low values [1].

The present contribution consists of two parts: one deals with the empirical facts extracted from the vibration measurements with existing bridges and another is the report of two model tests which were conducted to obtain some qualitative natures of the damping of bridge superstructures. The former is a kind of supplement to the previous paper [2] by two of the present authors. The accumulation of experimental data of damping is mostly necessitated for the more reliable dynamic analysis of structures, because the damping of structures should be relied upon empirical estimation.

2. VIBRATION DAMPING OF EXISTING BRIDGES

2.1 Vertical Vibration of Bridge Superstructures

Early experimental studies on the damping of bridges were made mostly for the vertical vibrations of superstructures in order to gather information on the impact effect of moving vehicles. Most of the available results are the damping of the fundamental mode of vibration. However, data from several recent tests seem to indicate that damping factors (or logarithmic decrement) associated with higher modes of vibration are of the same order as that of the fundamental mode. Though material damping of concrete is at least several times greater than that of steel, at present it is difficult to obtain any definite relation between the damping and the material used for bridge superstructure. This seems to suggest that the damping of bridge superstructure is mostly governed by the energy dissipation at joints, joint interfaces and supports. By plotting damping against span length it was found that the damping values of bridge superstructures with span lengths less than 40 m show larger scatter than those with span lengths

greater than 40 m and that the former are greater than the latter on the average [2]. This tendency can be seen in Fig. 1 in which data for suspension and cable-stayed bridges are shown separately from other types of bridges. Damping values of different modes of vibration were counted as independent data and those for torsional as well as vertical vibrations were included for the case of suspension and cable-stayed bridges. Simple averaging gives damping factor $h = 0.016$ (logarithmic decrement $\delta = 0.102$) for spans less than 40 m, $h = 0.013$ ($\delta = 0.084$) for spans greater than 40 m, and $h = 0.009$ ($\delta = 0.058$) for suspension and cable-stayed bridges. Fig. 2 shows the damping values of suspension and cable-stayed bridges versus their span lengths. The values are generally in a narrow range, $h = 0.003$ to 0.013 ($\delta = 0.02$ to 0.08), except for several cases. Though only estimated values are available for suspension bridges with longer span lengths, they also fall in the range mentioned above. A value of $\delta = 0.03$ is adopted for the structural damping of the suspended structures of long-span suspension bridges in Japan for the aerodynamic stability analysis.

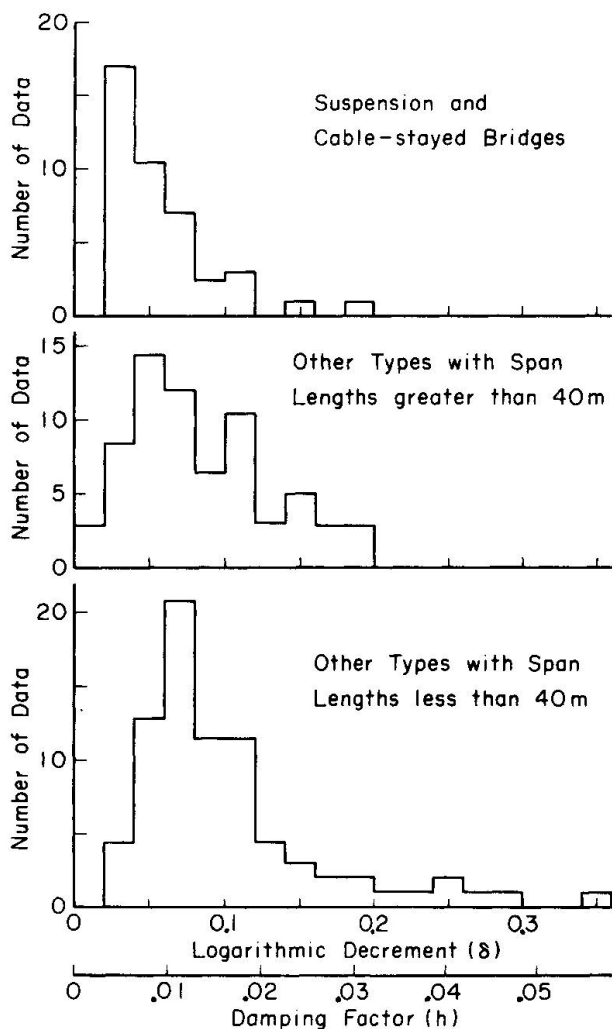


Fig. 1 Distribution of Damping Values of Bridge Superstructures

Fig. 2 shows the damping values of suspension and cable-stayed bridges versus their span lengths. The values are generally in a narrow range, $h = 0.003$ to 0.013 ($\delta = 0.02$ to 0.08), except for several cases. Though only estimated values are available for suspension bridges with longer span lengths, they also fall in the range mentioned above. A value of $\delta = 0.03$ is adopted for the structural damping of the suspended structures of long-span suspension bridges in Japan for the aerodynamic stability analysis.

2.2 Torsional Vibration of Bridge Superstructures

The damping value for torsional vibration has been believed to be generally higher than that for bending vibration in the same structure. In suspension bridges and cable-stayed girder bridges, however, the logarithmic decrements for both vibrations are found comparable each other [3], the data for other types of structure having short and medium span length are not available though.

2.3 Horizontal Vibration of Whole Bridge System

In the earthquake resistant design of bridge structures, the dynamic behaviors of a whole bridge system in horizontal directions play the most important role. In last fifteen years in Japan, a number of dynamic tests were carried out for bridge foundations, piers, and completed bridges. Emphasis in these tests were placed on the investigation of horizontal dynamic behaviors both in lateral and in longitudinal directions. Most of these tests were performed by using vibration generator mounted on a structure.

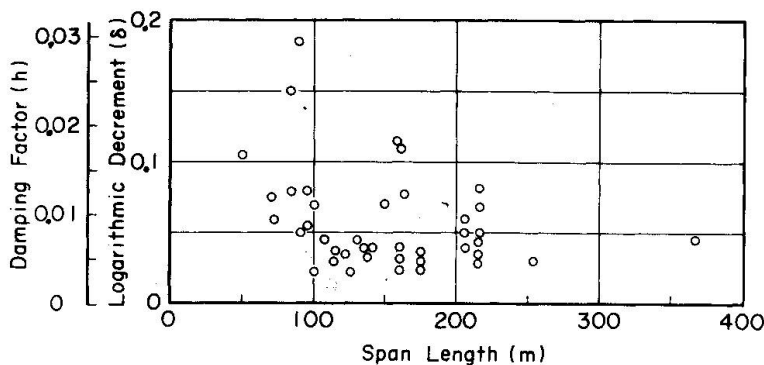


Fig. 2 Damping of Suspension and Cable-stayed Bridges vs. Span Length

In Fig. 3 are shown damping

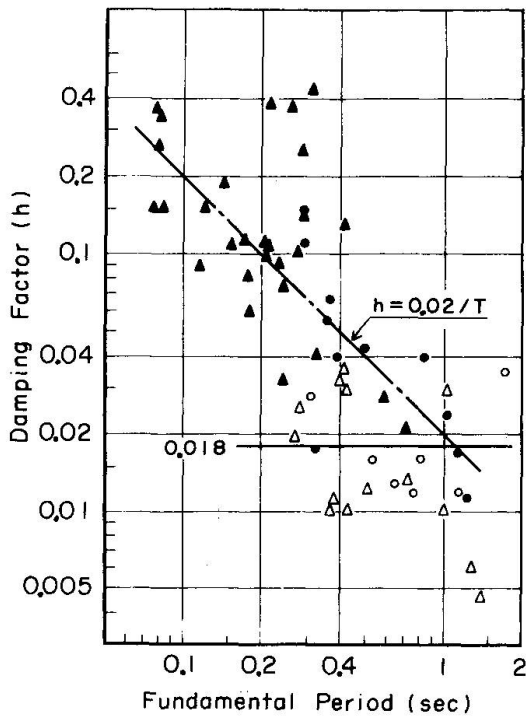


Fig. 3 Relation between Damping and Natural Period for Horizontal Fundamental Mode of Vibration (▲: Foundations and ordinary piers, ●: Bridges and ordinary piers, △: Tall piers with height greater than 25 m, ○: Bridges on tall piers)

completed bridge systems gave a relation between the damping and the period as

$$h = 0.0228 T^{-0.97} \tag{1}$$

which confirms the usefulness of the approximate formula

$$h = 0.02/T \tag{2}$$

proposed by Kuribayashi and Iwasaki for the estimation of damping factor of the types of structures mentioned above [4]. However, it should be noted that the deviations of actually measured values from the values calculated by Eq. (2) are often very great as shown in Fig. 4 indicating the complexed nature of damping mechanisms in actual structures. On the other hand, damping factors of tall piers and bridges on tall piers are not strongly dependent on natural periods. The simple average is $h = 0.018$ ($\delta = 0.116$) and the scatter of 20 data about the average is shown in Fig. 5.

For the dynamic analysis of flexible structures with long fundamental natural periods, it is often necessary to assume damping of higher modes of vibration. In

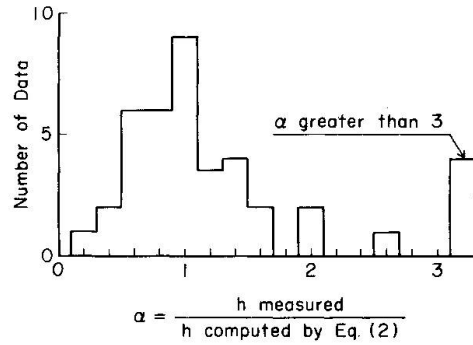


Fig. 4 Scatter of Data about the Line $h = 0.02/T$

factors of the fundamental mode of vibration for foundations, foundation-pier systems, and foundation-pier-superstructure systems. Most of the data in Fig. 3 were taken from Ref. [4] and twelve data from other sources were added. Data are divided into two groups, namely those for ordinary short piers and those for tall piers with heights greater than 25 m. There is a significant difference between the two groups of data though damping factors of bridge structures with fundamental periods longer than 0.4 sec are usually between 0.01 and 0.04 regardless of the types of piers. The least square fitting on the log-log basis for 40 data of foundations, ordinary foundation-pier and ordinary

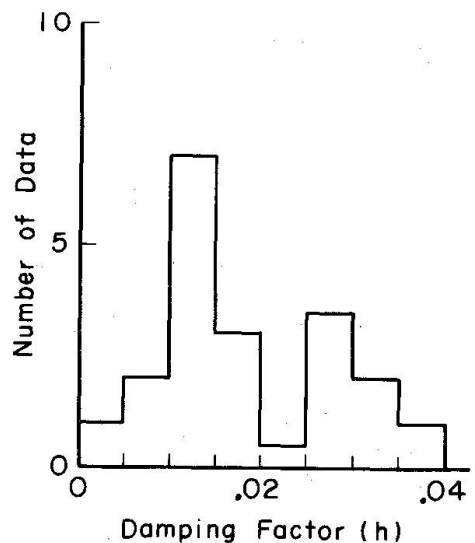


Fig. 5 Scatter of Damping Factors for Tall Piers and Bridges on Tall Piers

order to investigate the damping associated with higher modes of vibration, the ratios h_1/h_2 of damping factors of the two lowest measured modes are plotted in Fig. 6 against the ratios T_1/T_2 of the corresponding periods. It is difficult to find any definite relation between these quantities but most of the h_1/h_2 values are close to or slightly less than unity except for several cases. However, it should be borne in mind that a vibration generator cannot usually excite a mode in which deformation of the foundation in the ground dominates and for which damping may be substantially greater than the observed values.

Table 1 Standard Values of Damping Factors for Bridges

		Damping Factor (h)		
		Average	Minimum	
Superstructures in Vertical Vibration	Suspension and Cable-Stayed Br. (Torsional Vibr. Included)	0.009	0.005	
	Other Types	Span Length > 40 m	0.013	0.005
		Span Length < 40 m	0.016	0.005
Whole Bridge System in Horizontal Lateral and Longitudinal Vibr.	Bridges on Short Piers	$0.02/T$	$0.01/T$	
	Bridges on Tall Piers with Height Greater Than 25 m	0.018	0.01	

2.4 Standard Damping Values of Bridges

The standard damping values of bridges for engineering purposes were estimated from the results of the foregoing study and are summarized in Table 1. If a vibrational mode of a whole bridge system is known to be the one in which soil-foundation interaction effect is great, a larger damping factor may be assumed (possibly 0.1 to 0.2) for that particular mode even for bridges on tall piers.

3. FINDINGS FROM MODEL TESTS

3.1 Effects of Mode, Mass and Rigidity

Aiming mainly to know the damping characteristics of very higher modes of vertical vibration, a flexible suspension bridge model having a single span length of 8 m was used in the experiment. The effects of various factors, such as mass, flexural rigidity and supporting conditions of the stiffening girder, were also investigated.

When other conditions are the same, the following findings were obtained from the experiments:

1) The effect of mode The free vibration tests were conducted up to such a higher order of mode as having eighteen nodes. As seen in an example in Fig. 7, the

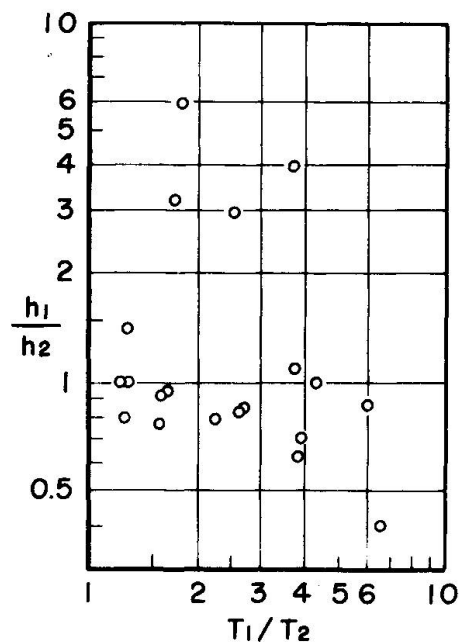


Fig. 6 Relation between h_1/h_2 and T_1/T_2

logarithmic decrement tends to increase at higher modes of vibration, especially in case the rigidity is large. However, this trend is somehow contrary to the previous tests with different models [2]. It seems that the damping value is sensitive to various other structural factors, but the present result appears to give general characteristics.

2) The effect of mass Increasing mass of the girder augments the logarithmic decrement, but quantitative analysis could not be made because of the shortage of data.

3) The effect of flexural rigidity In many cases less rigidity brought on less damping, but this tendency was not clear. The change in rigidity did not affect so much on the damping of symmetric modes and very higher modes of vibration.

4) The effect of amplitudes The damping values seem to increase with increasing amplitudes at higher modes of vibration. Judging from other data [3, 4], however, they are independent on the amplitude in the range of small displacement.

5) The effect of supporting condition The Coulomb's damping due to the movement of supports is said to play an important role in long-spanned bridges. Three cases were tested: both ends movable, one end pinned and both ends pinned. Distinct differences were not observed, but the case of movable support showed larger damping values particularly at lower asymmetric modes. It must be noted that the friction at movable bearings was very small in the present model.

Table 2 Results of Girder Test

Combination of device	Log. Decrement	Efficacy*
Without any device	0.034	
(1) Rubber shoe	0.064	○
(2) Rubber slide-plate	0.070	○
(3) Concrete block movable	0.096	○
(4) Stringer movable	0.050	△
(1) + (2)	0.074	×
(1) + (3)	0.097	×
(1) + (4)	0.109	○
(2) + (3)	0.108	△
(2) + (4)	0.120	○
(3) + (4)	0.072	×
(1) + (2) + (3)	0.081	×
(1) + (2) + (4)	0.181	○
(1) + (3) + (4)	0.078	×
(2) + (3) + (4)	0.117	△
(1) + (2) + (3) + (4)	0.141	△

* ○... good, △... moderate, ×... poor

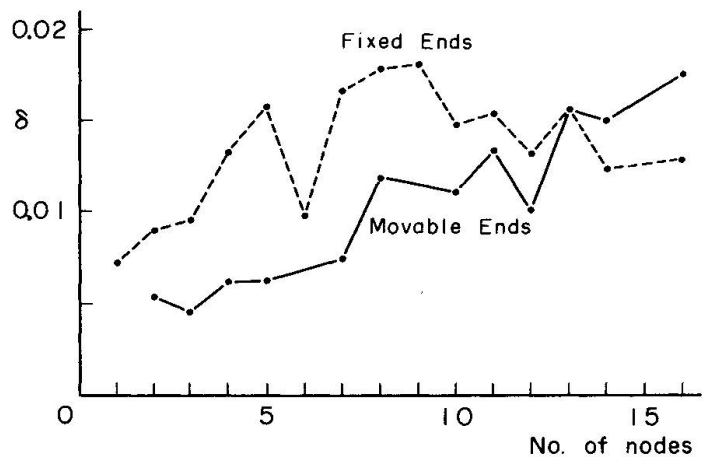


Fig. 7 Damping vs. Modes of Suspension Bridge Model

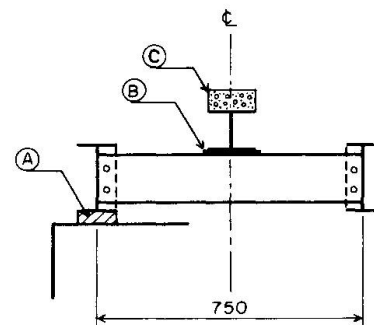


Fig. 8 Cross Section of Model Girder

3.2 Effects of Structural Assemblage

Making use of a simply-supported girder model, the section of which is as shown in Fig. 8, the effects of interface damping on the overall damping were tested. The arrangements for this purpose are as follows, referring to Fig. 8:

Ⓐ Bearings of girder Three types of supporting conditions: both ends movable, one end fixed and both ends fixed, and two kinds of bearing materials: rubber and iron plate, were compared in their

combination.

- ⓑ Stringer With and without a stringer. When with it, the stringer was placed movable on the slide-plate of rubber or gunmetal attached to cross-beams, and the torque to tighten bolts connecting the stringer was also varied.
- ⓒ Concrete blocks With and without concrete blocks on the stringer. When with them, the concrete blocks were either connected or not connected with the flange of girders.

The results of free vibration tests indicate that such devices as increasing the friction between different structural parts and contributing to energy dissipation, can augment the overall damping of structure to some extent, but their combination does not always bring about the algebraic superposition of each effect. These situations are illustrated in Table 2.

REFERENCES

- [1] Katayama, T.: A Review of Theoretical and Experimental Investigations of Damping in Structures, UNICIV Rep. No. 1-4, Univ. of New South Wales, Australia 1965.
- [2] Ito, M. and Katayama, T.: Damping of Bridge Structures, Trans. Japan Soc. Civil Engr., No. 117, 1965.
- [3] Ohkubo, T., Narita, N., Enami, Y., et al.: Technical Notes, ST-1, 3, 4 and 8, Public Works Res. Inst., Ministry of Construction, Japan 1968/9.
- [4] Kuribayashi, E. and Iwasaki, T.: Earthquake Resistant Design of Bridges (III)-- Experimental Studies on Vibrational Damping of Bridges, Report of Public Works Res. Inst., Ministry of Construction, No. 139-2, Japan 1970.

SUMMARY

The standard damping values of bridges for engineering purposes are estimated from the results of survey on existing bridges. Furthermore, two model tests were conducted to know the effects of various factors on the overall damping of superstructures. The damping values seem to be generally increased, but not so remarkably, with increasing order of modes and mass of structure. The influence of interface friction between different structural elements is also reported.

RESUME

Les valeurs d'amortissement courantes des ponts du génie civil sont estimées grâce aux résultats des expertises faites sur des ouvrages existants. De plus, on a réalisé deux essais sur modèle pour connaître les effets des différents facteurs sur l'amortissement global des superstructures. Les valeurs d'amortissement semblent généralement augmenter, suivant un ordre croissant selon le type et la masse de l'ouvrage. On montre aussi l'influence des frottements internes entre les différents éléments de la structure.

ZUSAMMENFASSUNG

Die Standardwerte für Brückendämpfung zu Ingenieurzwecken werden aus Resultaten von Beobachtungen an bestehenden Brücken geschätzt. Ferner werden zwei Modell-Versuche beigelegt zwecks Erforschung der Auswirkung verschiedener Faktoren auf die globale Dämpfung des Ueberbaus. Die Dämpfungswerte scheinen generell, jedoch nicht sehr ausgeprägt, mit zunehmender Ordnung der Schwingung und der Masse des Tragwerkes zu wachsen. Der Einfluss der inneren Reibung zwischen verschiedenen Bauteilen wird ebenfalls behandelt.

Studies on Vibration Damping of Steel Structures

Etudes sur l'amortissement des vibrations dans les structures en acier

Studie über Dämpfung von Vibrationen an Stahltragwerken

Yoshikazu YAMADA
 Professor of Structural Engineering
 Department of Civil Engineering
 Kyoto University
 Kyoto, Japan

1. Introduction

Properties of vibration damping of actual structures were mainly determined by field observations. The investigations, however, are usually limited to vibrations with very small amplitude. The damping properties necessary for structural design for dynamic loads must be corresponded to the actual loading conditions of the structures. Theoretical investigations, frequently, give more valuable information on this than limited field investigations.

In this paper, damping properties of steel structures, especially friction joints, within the elastic limit of the material were investigated by theoretical mean, and the relations between damping constants and amplitudes were obtained and given by specific formula. The model experiments were also done to examine the theoretical results.

If the effects of all sources of vibration damping are mutually exclusive, energy dissipation in one cycle of oscillation is given as,

$$\Delta W = \Delta W_1 + \Delta W_2 + \Delta W_3 + \cdots + \Delta W_n \quad (1)$$

where, ΔW_i indicates energy dissipation due to a specific source of vibration damping. If a specific number of sources in Eq. (1), say j , can be evaluated by theoretical or experimental means, energy dissipation obtained by the relation,

$$\underline{\Delta W} = \Delta W_1 + \Delta W_2 + \cdots + \Delta W_j \quad (2)$$

is always a lower bound of the real value ΔW . Damping constant computed by the equation,

$$\underline{\beta} = \frac{1}{4\pi} \frac{\underline{\Delta W}}{W} \quad (3)$$

is adoptable as a safe side value for practical dynamic design instead of real value β . Evaluation of specific source of vibration damping is important in this situation.

2. Preliminary Experiment

Fig. 1 shows the amplitude decay curves for two different model beams.⁽¹⁾ The first model has welded cross section and the vibration damping of this model is mainly due to material damping. The other model, the riveted beam, shows far rapid decay of amplitude since the damping due to mechanical friction is included in the model. Fig. 2 is more lucid expression of the results showing the relation between the damping constants and amplitudes. The riveted beam shows higher order property of damping than linear damping as in welded beam. If the source of damping is Coulomb type the damping constant and amplitude relation has to be decreased with amplitude as shown in the fine dotted line in Fig. 2.

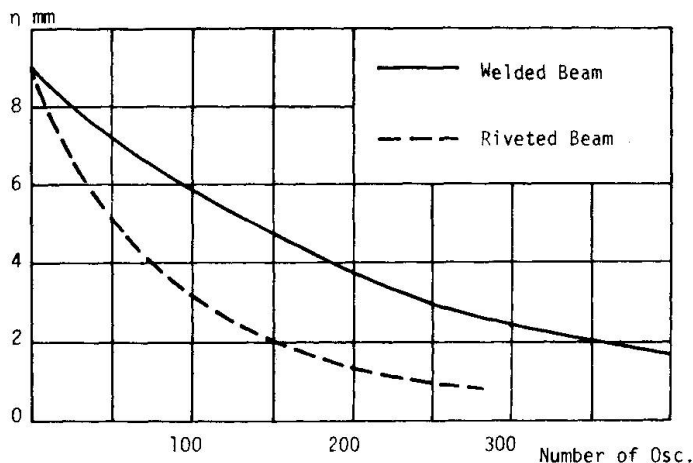


Fig. 1

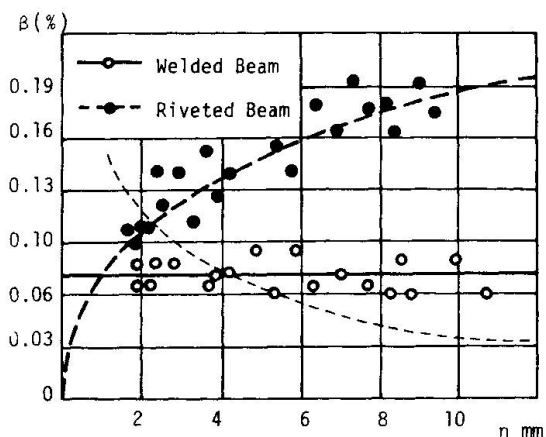


Fig. 2

According to the results given in Fig. 2, damping due to mechanical friction in riveted beam shows higher order damping than material damping and is not pure Coulomb damping. Damping due to mechanical friction of joints is explained by investigating the mechanism of energy dissipation as shown in the following.

3. Damping of Friction at Joint

Two kinds of method of analysis to obtain energy dissipation from friction joints are available. The first method was given by Pian and Hallowell⁽²⁾ investigating the damping effect of a simple built-up beam. In this method, external load and deformation relationship during one cycle of loading was investigated, and the energy loss during the cycle was obtained. In the other method, given by Goodman and Klumpp⁽³⁾, the energy loss was obtained directly by integrating partial slip multiplied by friction force.

Energy dissipation due to a cycle of loading for specific types of structural member and loading is investigated in this study by the first method, and the following results were obtained.

For the Case (a), Fig. 3,

$$\Delta W = \frac{48 \kappa' M_{\max}^3}{(1+2\kappa)^2 EI_c q_m t}$$

For the Case (b),

$$\Delta W = \frac{72 (m+m^2)^2 F_{\max}^3}{3(1+2\kappa)^2 EI_c q_m t} \cdot \left[\frac{(c+e)^3}{(1+\phi_0)^2} + \frac{(c-e)^3}{(1-\phi_0)^2} \right] - \frac{72 (m+m^2)^2 c^3 F_{\max}^3}{4\kappa^2 EI_c (1+2\kappa) q_m t} \cdot \left[\frac{1}{1+\phi_0} + \frac{1}{1-\phi_0} \right]$$

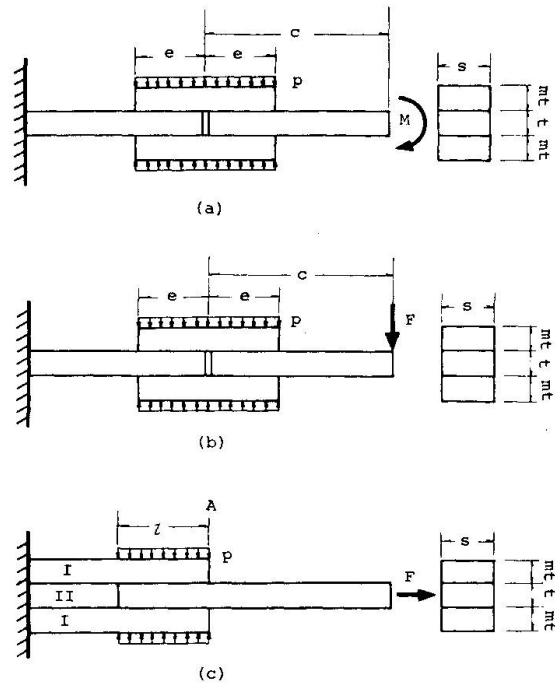


Fig. 3

where,

EI_c : equivalent stiffness

q_m : critical friction force

$$\kappa = 3m + 6m^2 + 4m^3$$

$$\kappa' = \frac{m+m^2}{\kappa^2} [2(m+m^2)^2 \kappa^2 - \{1+(2-m-m^2)\kappa\}], \quad \phi_0 = \frac{6(m+m^2)F_{\max}}{(1+2\kappa)q_m t}$$

For Case (c),

$$\Delta W = \frac{2F_{\max}^3}{3k_2 q_m} \frac{1-3k+3k^2}{1-k}$$

where, $k = k_2/(k_1+k_2)$, $k_1 = A_I E_I$, $k_2 = A_{II} E_{II}$.

Other types of members were also investigated, and the results almost the same.

The important point of these results is that the dissipation energy W is proportional or approximately proportional to the cubic power of the maximum external force. Since the maximum deflection is proportional to the maximum external force in elastic structures the energy dissipation is proportional to the cubic power of the maximum deflection. Total energy, strain and kinetic energy, stored in the vibrating structure is proportional to the square of the maximum deflection. Damping capacity and damping constant are, therefore, proportional to maximum deflection and do not maintain a constant value during vibration in this case.

4. Experimental Studies

Experimental studies were done to investigate damping constant deflection relation in structures with joints using simple models. The models used in these studies are cantilever beams with bolted connections. The model without joint is also used for reference. Normal pressure in contact of the friction joints was controlled by means of torque value of the bolts. The joints in the models are located in various position.

Fig. 4 shows amplitude decay curves for the beam with bolted joint, $T = 1000 \text{ kg-cm}$, (a) and for the beam without joint (b). Fig. 5 shows the variation of damping constants due to the position of joints. Four different types of beams are compared in the figure. Damping constants for type D is almost the sum of those of type B and type C.

Fig. 6 shows the effects of normal pressure of the joints. The normal pressure is approximately proportional to the torque value shown in the figure. The result is well coincide with theoretical investigation.

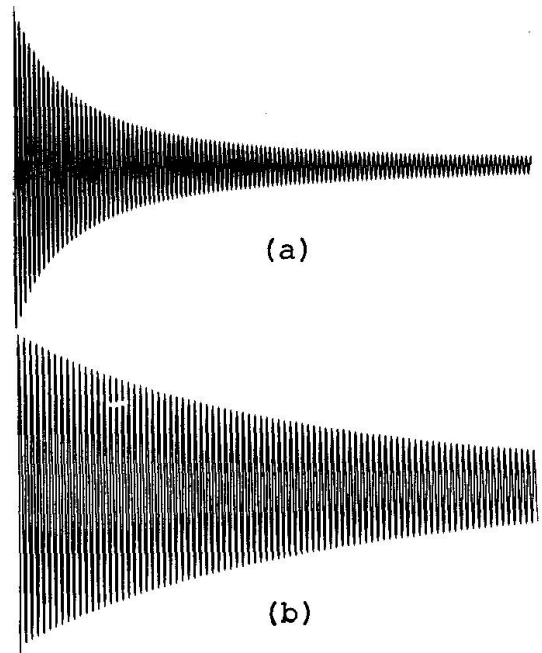


Fig. 4

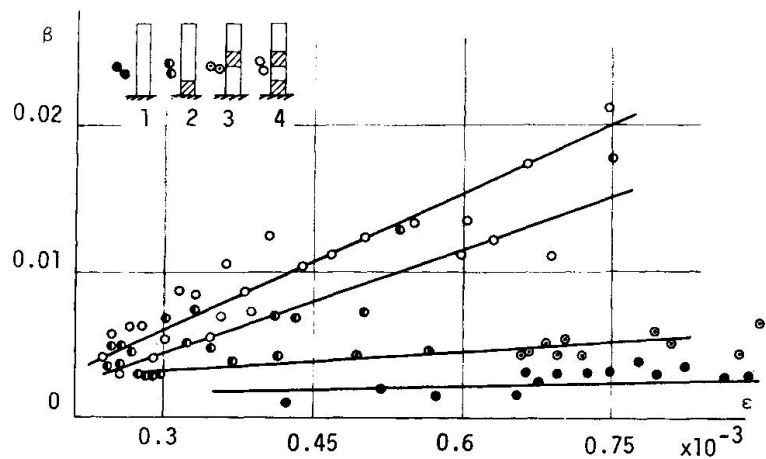


Fig. 5

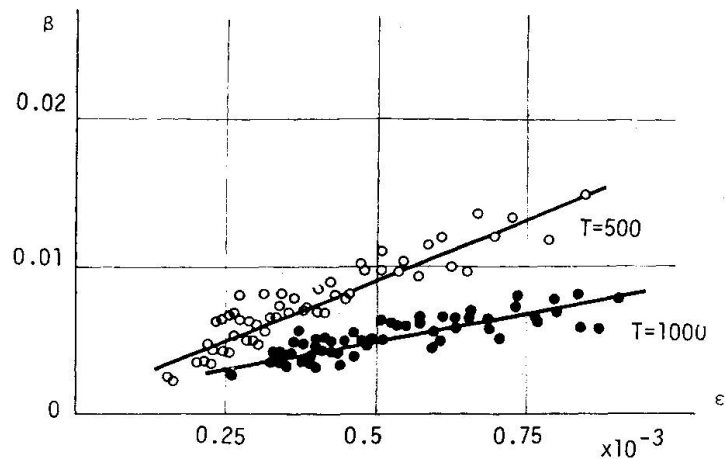


Fig. 6

5. Damping of Illustrative Model Beams

Dissipation energy from the beam with splice joints as shown in Fig. 7 during one cycle of vibration is given as follows.

$$\Delta W = \frac{8}{EI} \left[\frac{2\lambda^2 M_{omax}^3}{3(1+\lambda)^2 q_m h} + q_m h \left\{ \frac{2(1+\lambda) q_m h e^3}{3} - e^2 M_{omax} - \frac{2(1+\lambda) q_m h e + M_{omax}}{3} \left(e - \frac{M_{omax}}{(1+\lambda) q_m h} \right)^2 \right\} \right]$$

where, $\lambda = 2I/(Ah^2)$

Assuming the numerical values $l = 10$ m, $e = 500$ mm, $h = 1000$ mm, $t = 20$ mm, $I = 56 \times 10^4$ cm⁴, $q_m = 3600$ kg/cm, and $E = 2.1 \times 10^6$ kg/cm², and the mode shape for the n -th order vibration as

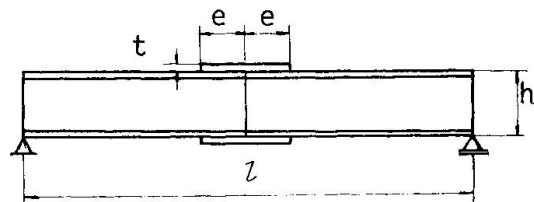


Fig. 7

the damping constant is given, approximately, as a straight line (a) in Fig. 8. If the beam has two splice joints at $l/3$ and $2l/3$ sections the damping constant is given as a straight line (b) in Fig. 8.

$$\eta = \eta_0 \sin \frac{n\pi x}{l}$$

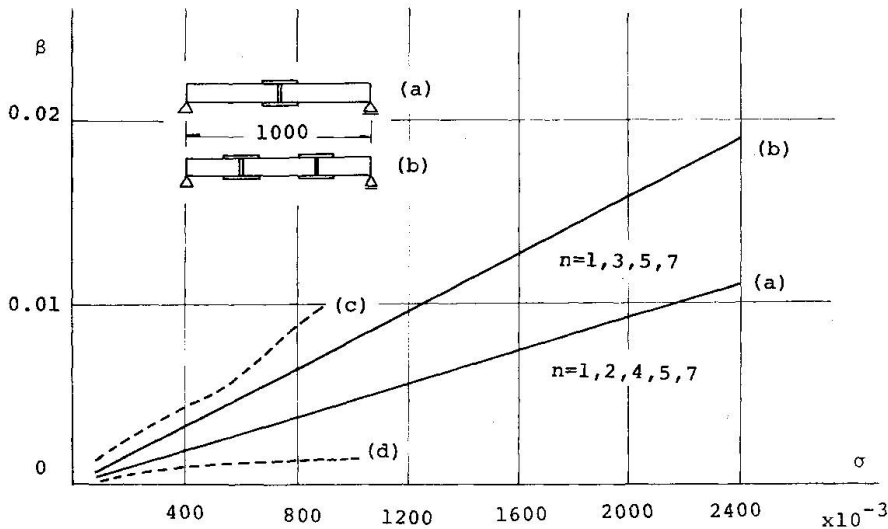


Fig. 8

Lines (c) and (d) in Fig. 8 are the experimental results obtained by U. S. Bureau of Public Roads⁽⁴⁾ for the truss type structure with bolted joints (Line (c)) and the solid beam without joint (Line (d)). Both models have approximately 10 m span length.

6. Conclusion

Properties of vibration damping due to the friction at joints of steel structures were investigated by theoretical and experimental means. Damping constant due to joint friction increases with vibration amplitude. This effect must be considered in the dynamic analysis and design of steel structures.

References

- (1) Yamada, Y., On the vibrational Damping of Structural Steel Beams, Memoirs of the Faculty of Eng., Kyoto Univ., Vol. 19, No. 1, 1957
- (2) Pian, T. H. H., Structural Damping of a Simple Built-up Beam with Riveted Joints in Bending, Jour. of Appl. Mech., Vol. 24, No. 1, 1957
- (3) Goodman, L. E. & J. H. Klumpp, Analysis of Slip Damping with Reference to Turbine Blade Vibration, Jour. of Appl. Mech., Vol. 23, 1956
- (4) Teller L. W., & E. G. Wiles, Tests of Structural Damping, Public Roads, Vol. 27, No. 10, 1953

SUMMARY

Structural damping due to friction at the connections of steel structures were investigated by theoretical and experimental means. Non-linear properties of damping were obtained even within the elastic limit of the material. Practical application of the results to actual simple structures was discussed.

RESUME

L'amortissement structural dû à la friction des connexions de structures en acier a été examiné par voie théorique et expérimentale. Des phénomènes non-linéaires d'amortissement ont été obtenus même entre la limite d'élasticité du matériau. On a discuté l'application pratique des résultats sur le cas de structures simples.

ZUSAMMENFASSUNG

Strukturelle Dämpfung infolge Reibung an den Verbindungen von Stahlbauten wurden theoretisch und experimentell untersucht. Nichtlineare Dämpfungserscheinungen wurden selbst innerhalb der Elastizitätsgrenze des Materials beobachtet. Es wurde die praktische Anwendung der Ergebnisse auf einfache Bauwerke diskutiert.

Model Tests on Structural Damping in Bridges

Essais sur modèles de l'affaiblissement structural des vibrations dans les ponts

Modellversuche über die strukturelle Dämpfung in Brücken

S. MENDEL

Dr. eng., major lecturer
of Silesian Technical University
Gliwice, Poland

1. Introductory

The vibration damping coefficient of structures is many times greater than that of small specimens, when the same material was used. Furthermore, the damping data vary in wide limits, depending strongly on tested object's structural characteristic / see Table 1 /.

Material damping represents only a part of the global damping. The remaining part, in most cases a greater one, may be treated as a result of non-material damping factors.

Table 1

Type of bridge	Log. decrement of damping		$\frac{\max}{\min}$
	min	max	
reinforced concrete	0,182	0,490	2,69
prestressed concrete	0,099	0,310	3,14
steel	0,061	0,161	2,64

This phenomenon, known as structural damping effect, encloses the total influence of spatial material distribution in the structure, mutual connections of members as well as the technical state of structure.

When the possibility of structural form modifications is nearly unlimited, some examples only can be given. These are, statical scheme including, the shape and size of bridge cross-sections, type and number of connections, the surface-structure conjointment as well as the type of bearings.

In contrast to the material damping, where some hypothesis, the numerical data too, are known, the structural damping is till now not very well recognized. Unfortunately none of mentioned above structural influences can be excluded from the global damping values, when existing bridges are dynamically tested. This interesting problem, which could be useful for pre-evaluation of the bridge dynamical properties, seems to be suitably solved, when testing the adequately constructionally adjusted big models.

Such tests have been undertaken by the author in Silesian Technical University.

2. Tests description.

The influence of some structural variations in tested models was investigated, namely: bearing type, number and stiffness of the floor beams as well as the skew angle. The participation of both material and structural dampings in the global damping was analysed. The effect of successively increasing initial dynamic displacement was enclosed with test programme too.

Thirty-five steel beams in single- and double-beam systems were tested, when steel of normal structural standard was used.

The basic model element was a single welded I-beam of 3,0 m span /Fig. 1/. Two main beams joined transversally with a number of floor beams, formed a simple double-beam bridge gridwork. The number of floor beams increased from two to five /Fig. 2/. In one of the tested series the floor beam/main girder stiffness ratio was successively decreased from 3,0 to 0,03 /Fig. 3/. The skew angle varied every 15° in limits from 45° to 90° , /Fig. 4/.

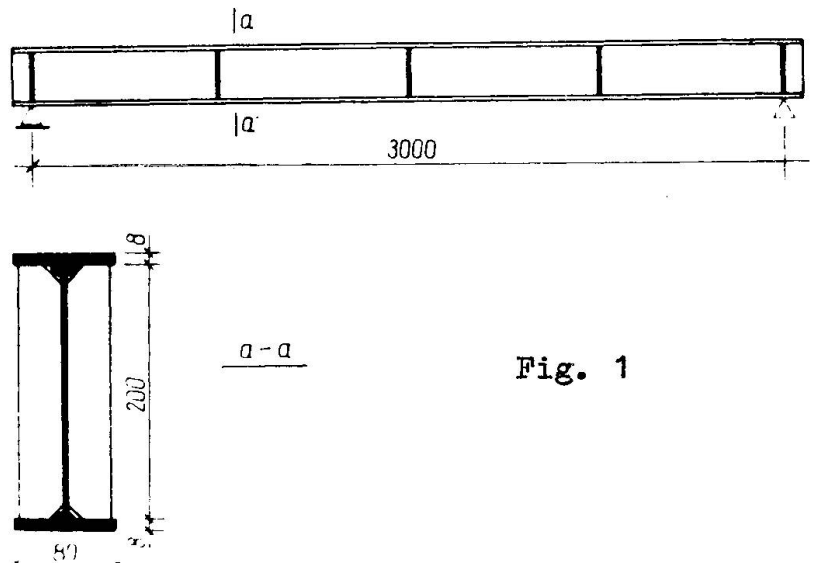


Fig. 1

Six types of bearings were used. A, B, C, D, E, F - types respectively: steel plate bearing with and without bituminous pad, steel tangential bearing, steel roller bearing, two- and five-layered steel-rubber bearings. Identical denotations are used at Fig. 5.

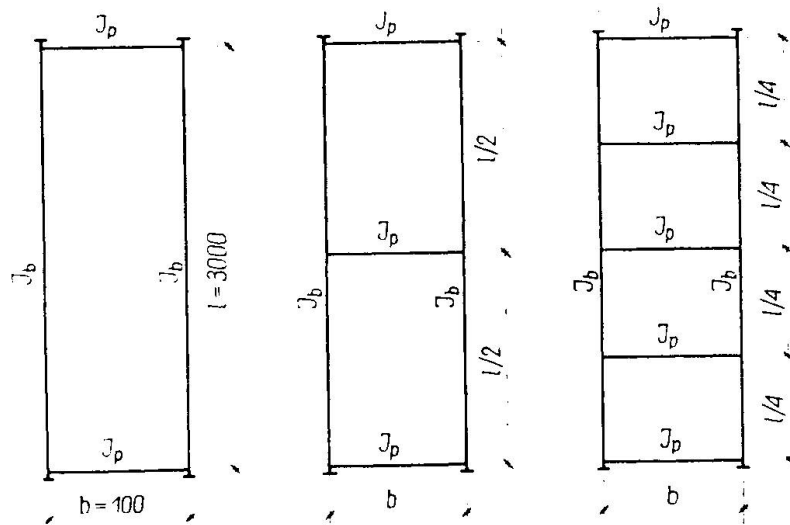


Fig. 2

The single - beam models were used only for bearing effect test. Double-beam models uniformly supported with tangential and roller bearings, served for the testing of remaining , enclosed by programme , structural effects.

When massive concrete test stand was used, any undesired distortion of results was practically out of the

question.

The vibration source was a single dynamic impulse, caused by the rapid release of initially deflected / $y_0 = 1-5 \text{ mm}$ / and with dial indicators controlled test beam. Vibrograms of the free damped

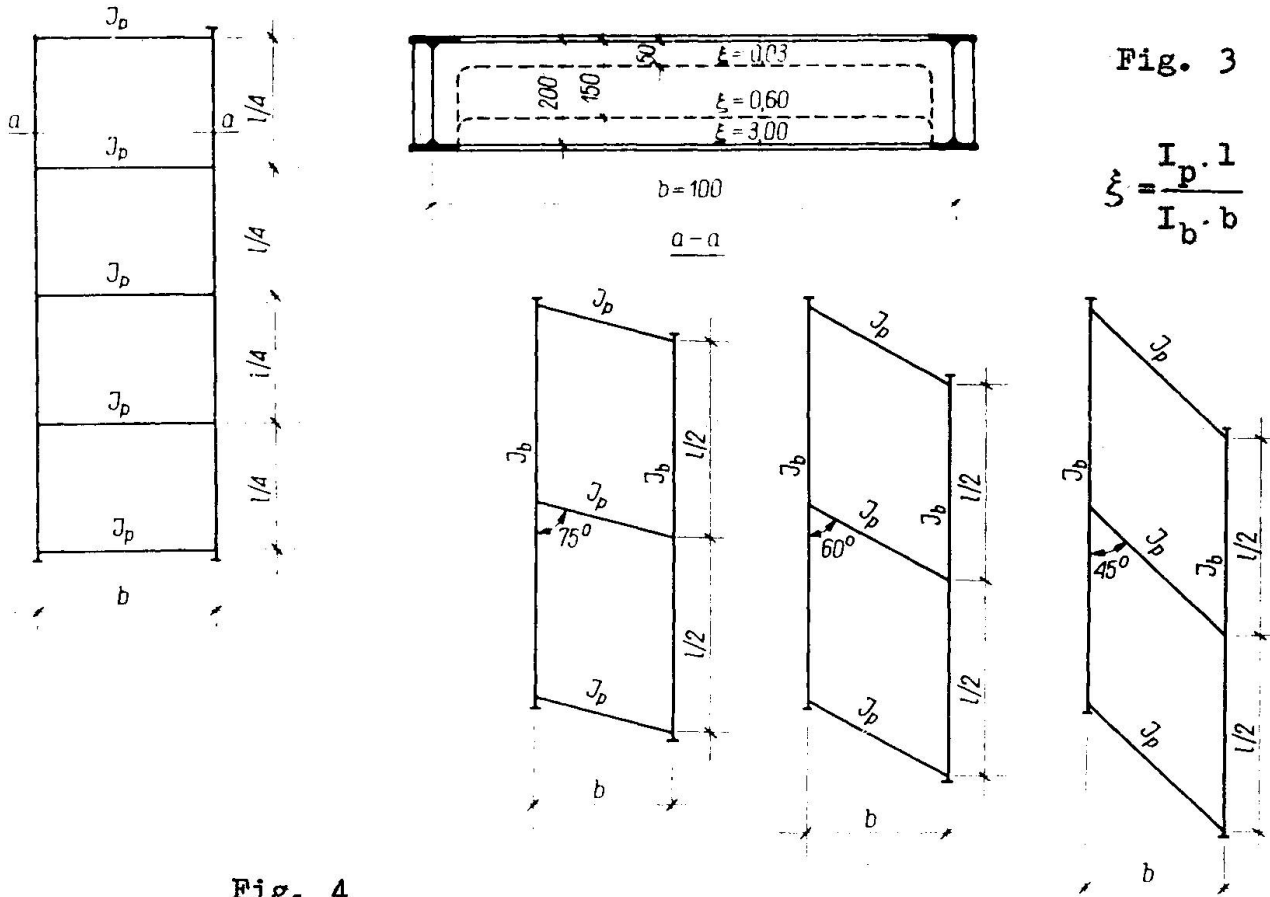


Fig. 3

$$\xi = \frac{I_p \cdot l}{I_b \cdot b}$$

Fig. 4

vibrations were recorded with Hottinger s set.

3. Test results.

Logarithmic damping decrement, obtained from the vibrograms analysis, was intended for comparison of the damping properties of each separate tested model.

These empiric data represent doubtless the global damping too. The subtracting of the mean value of the material damping decrement for used steel standard /0,008 - proved by other authors/

enables evaluating of structural part of summarized effect corresponding with the characteristic of the tested model.

Results are given graphically in Fig. 5 and Fig. 6 .

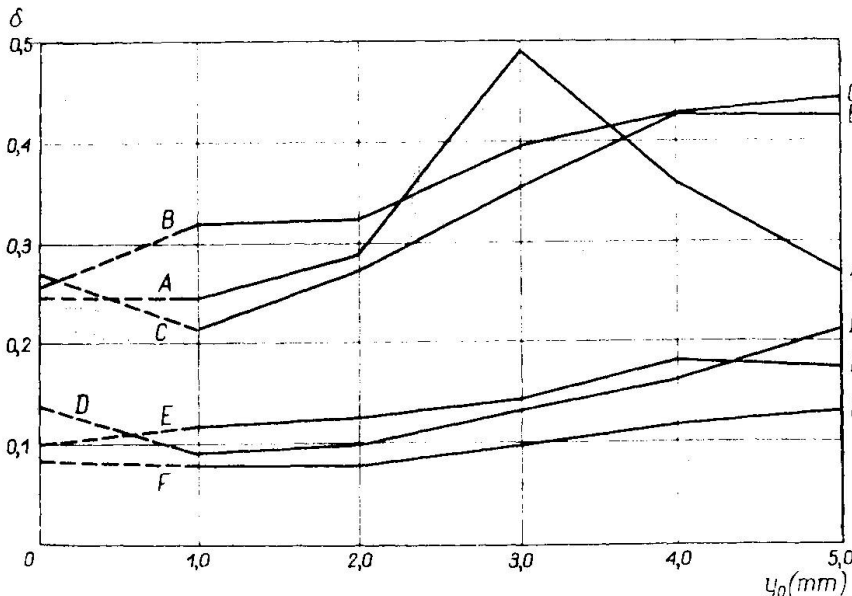


Fig. 5

Denotations-see text

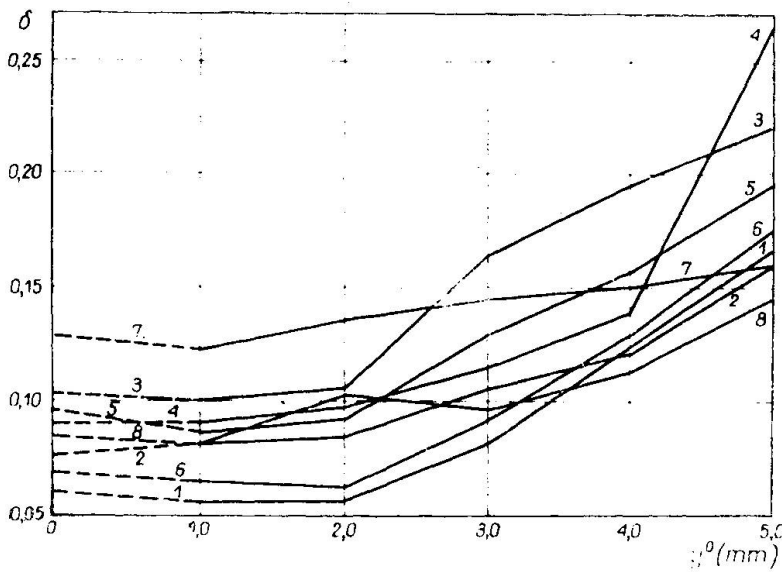


Fig. 6
 Denotations:
 δ - log. decrement
 y^0 - initial deflection
 ξ - see Fig. 3
 n - number of floor beams
 α - angle of skewing

1, 2, 3 - $n=5$
 $\alpha=90^\circ$
 ξ = resp. 3,0; 0,6; 0,03

4, 5 - n = resp. 3; 2;
 $\alpha=90^\circ$
 $\xi=3,0$

6, 7, 8 - $n=3$
 α = resp. 75° ; 60° ; 45° ;
 $\xi = \text{const.}$

4. Conclusions.

When omitting the peculiar interpretation of the individual diagrams, some more general conclusions can be drawn.

The constructional form's effect on damping is evident and considerable.

In tested cases this effect reaches 70 - 90 % of the global damping.

The simple - formed bearings, low stiffness of the transversal beams as well as the angle of skew near to 90° result in relative increasing of the damping properties.

Remarkable is an evident increase of the damping accompanying the increase of initial beam deflection.

Considerable structural damping effects are to be expected especially in the short - span and primitive - supported bridges. In these cases the structural damping effect could be treated as the dominant one.

The damping effect of the rubber bearings doesn't exceed the one recorded for steel roller bearings.

Tests presented here concern hardly a limited number of possible form modifications in tested models. The too poor number of data does not give full enough

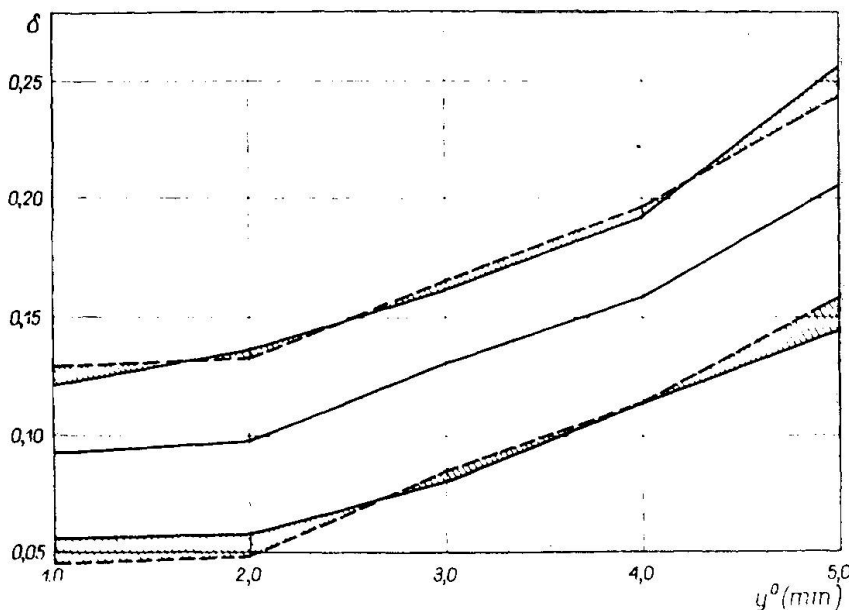


Fig. 7

representation of a tested phenomenon. The run of the envelope curves for all tested cases /Fig. 7/ indicates, however, some interesting regularities. They may give assumption, that in the mathematical analysis of free damped vibrations the global damping forces should be divided into material and structural parts. The material factor should represent of "specific damping" undependent of the structure's shape and sizes. These and the other constructional features should be described by the functional quantity enclosing in general the spatial material's distribution effect.

When analysing other forms of vibrations, additional damping forces should be still taken into account, especially these resulting from the vehicle / bridge co - action.

SUMMARY

Contribution of structural damping to the global one in the bridge systems has been analysed. The procedure results and interpretation have been given. The damping effect of bearings, stiffeners and skewing have been tested. In some cases the effect of structural damping in bridge structures can be the dominant one.

RESUME

On a étudié le part d'affaiblissement dans l'affaiblissement global de la construction des ponts. On décrit les essais, les résultats et leur interprétation. Les influences d'affaiblissement des appuis, des entretoises et du biais des ponts ont été comprises dans le programme d'essai. Dans quelques cas l'influence de l'affaiblissement structural peut s'avérer décisive.

ZUSAMMENFASSUNG

Es wurde der Dämpfungsanteil in der globalen Dämpfung der Brückenkonstruktionen untersucht. Der Testvorgang, die Ergebnisse und ihre Interpretation werden angegeben. Die Dämpfungseinflüsse der Lager, der Querträger sowie der Brückenschiefe wurden in das Versuchsprogramm einbezogen. In manchen Fällen kann sich der Einfluss der Dämpfung in der Brückenkonstruktion als massgebend erweisen.

Leere Seite
Blank page
Page vide

External Damping as a Means of Controlling Vibration in Modern Roofs

L'amortissement extérieur comme moyen de contrôle des vibrations dans les toitures modernes

Äussere Dämpfung zum Zweck der Vibrationskontrolle in modernen Dächern

J. BOBROWSKI
Senior Partner
Jan Bobrowski and Partners
London, England

J.A.C. CRAMER
Managing Director
Cementation (Muffelite) Ltd.
London, England

Professor Wakabayshi has described the favourable effect of damping by energy absorption in connection with seismic structures.

1. Introduction

Roof structures, and in particular cantilever structures, such as Grandstand roofs, are especially susceptible to wind excited vibration. Wind provides exciting forces and a roof has to be restrained in order to increase its fatigue life. The magnitude of vibration can be controlled either by increasing the stiffness of the roof or by adding damping to the system. The addition of damping is generally preferable since the resulting structure can be lighter and consequently more economical. In addition the energy produced by the wind forces is dissipated within the damping system rather than the roof itself and consequently the parts designed to absorb and dissipate energy, namely the dampers, do the work rather than this being undertaken by the structure of the roof.

The purpose of this paper is to illustrate how modern thin roofs are designed and also how damping can be incorporated into these designs so as to ensure satisfactory life whilst imposing minimal limitations on the overall configuration. The object of the paper is to describe three methods of applying damping to roof structures of different forms and show how the damping elements can be incorporated without imposing limits on either the structural or the architectural aspects of the basic solution. This problem has assumed greater importance with the introduction of prestressed concrete since the monolithic and light structures that result possess little internal damping.

The authors describe damping arrangements in two completed structures and one detailed project.

The excitation of the roof can be caused by two factors, one being the gust frequency of wind which can generate a low frequency vibration and secondly the higher frequency vibration that can be excited due to the effect of the aerodynamics on the roof; usually brought about by the build-up of vortices and the rate of shedding of these vortices from the leading and trailing edges of the roof. This characteristic is well known in aerospace technology and is the prime cause of flutter of aircraft wings.

2. Cantilever Roof for Doncaster Racecourse Grandstand, England

The roof, cantilevering 17 m, and carrying a structure weighing 27 tons accommodating Judges and Television facilities at the end of the cantilever, was completed in 1969. Lightweight concrete was used as the cranes available had limited carrying capacity¹.

Figures 1 and 2 show sections of the roof element and grandstand structure. Figure 3 shows a photograph of the front of the grandstand, with the Judges complex at the tip of the cantilever. Figure 4 shows a view of the vibration isolation and damping system.

It had been discovered on another racecourse with a similarly positioned Judges complex that due to wind excited vibration a great deal of discomfort was felt by those occupying the complex and severe limitations were imposed upon cameramen operating television and press cameras due to the oscillation of the structure.

The design was first conceived to provide a vibration isolation system for the Judges Box so as to eliminate the transmission of vibration from the roof to this complex, and additionally to ensure even load distribution across the nine supporting elements.

The natural frequency of the roof was determined to be of the order of $2\frac{1}{2}$ Hz and consequently it was decided to support the entire Judges/Press complex on large helical spring vibration isolators with a vertical resonant frequency of 0.8 Hz. The structure is located by a parallelogram linkage so as to permit movement in a vertical plane only and eliminate any rocking that would result had this additional restraint not been provided. With this system any vibration within the roof is effectively eliminated from the boxes and consequently no discomfort or limitation of use is experienced in the complex.

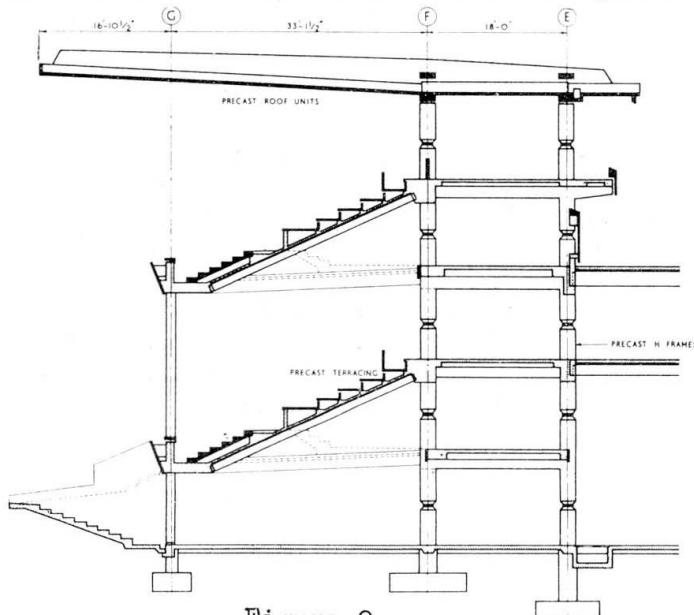


Figure 2.

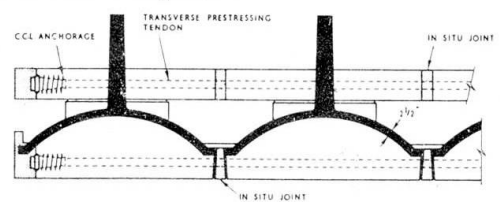


Figure 1.

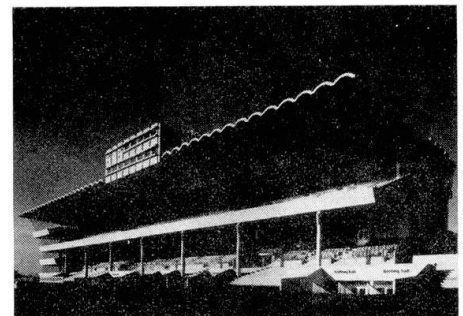


Figure 3.

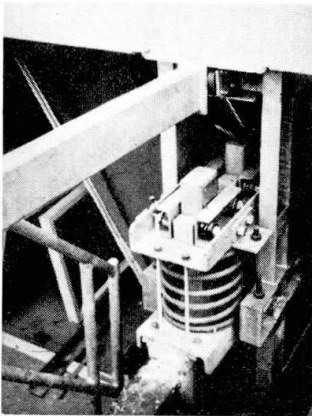


Figure 4.

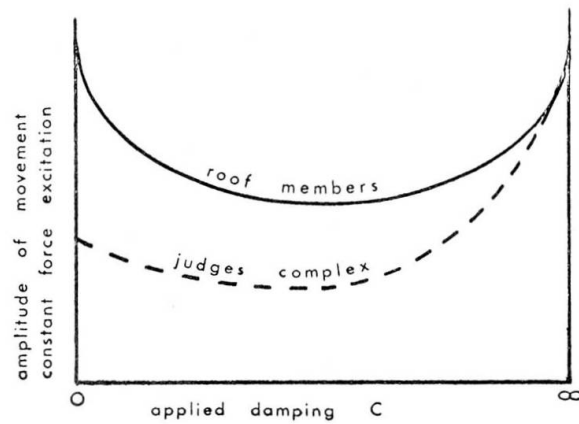


Figure 5.

Friction damping elements are interposed between the roof structure and the box complex. In the first instance these dampers restrict the build-up of amplitude of vibration caused by any excitation within the boxes at or near the resonant frequency of the spring system which could be caused by movement of personnel within the boxes or wind gust conditions. These frictional dampers are adjustable and are adjusted to give optimum results.

The complete system also serves as an auxiliary mass damper and will therefore reduce the amplitude of movement of the roof itself. This reduction of movement of the roof which is illustrated in Figure 5, will also reduce the amplitude of movement of the box complex since the input vibration level is lower.

From the point of view of the roof members alone the effective damping force should be a maximum to reduce movement, however as the damping increases so the transmission of vibration from the roof to the box also increases. The damping was adjusted by experimental methods to achieve optimum conditions whereby the transmission to the box when the roof is excited by wind forces is reduced to a minimum and also the dissipation of energy from the roof is at a maximum.

Since the cantilever beams supporting the Judges Box carry the mass at the end seismically supported, the resonant frequency of these beams is higher than would be the case had the boxes been rigidly fixed at the tip, therefore the overall dynamic stiffness of this part of the roof is greater and consequently the life of these members will be extended.

3. Grandstand at Sandown Park, England

In this case the roof design relies on stainless steel suspension cables. Figure 6 shows a cross section of the grandstand structure. The construction consists of prestressed concrete members positioned 6 metres apart and linked with lightweight transparent plastic roofing (Figure 7.).

It was decided that the only practical place for the positioning of any damping devices was at the highest point of the supporting cables, and consequently the bearing blocks that carry the cables through the centre pillars are located on a friction material designed so that as the roof vibrates, the cables will stretch and the bearing block will move horizontally by half the amount of the extension (Fig.8). The degree of damping in this instance is not as great as at Doncaster, but it is adequate to reduce the movement of the roof to an acceptable level. Enough safety is available for high strength stainless steel of lower fatigue limit than that of carbon steel for satisfactory performance.

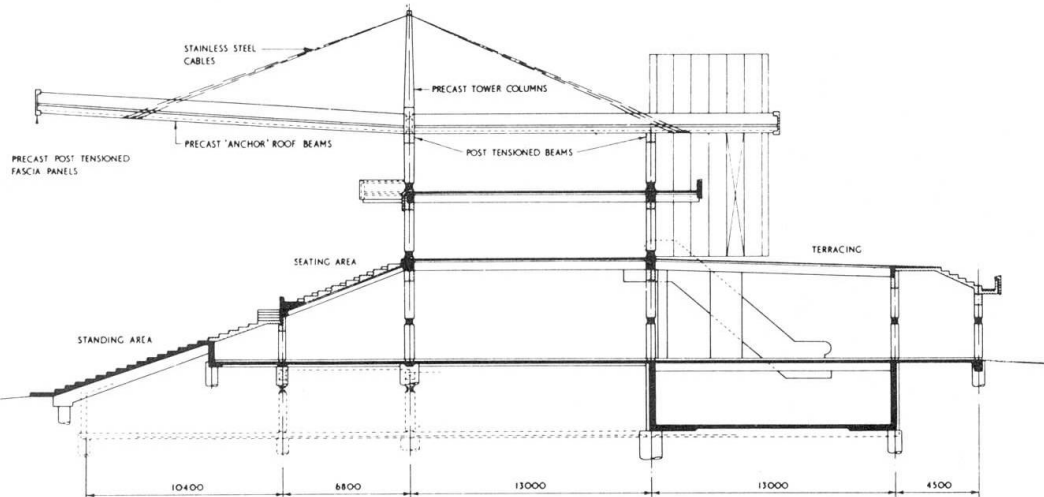


Figure 6.

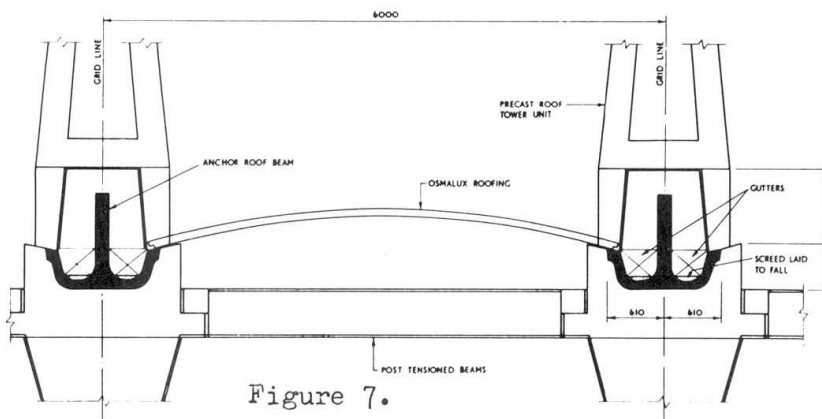


Figure 7.

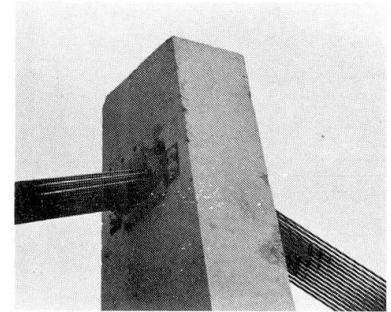


Figure 8.

This application of damping is particularly interesting as it shows how it was incorporated within the design whilst imposing negligible extra cost and no change to the overall configuration of the structure. The additional cost of providing damping was only a few hundred pounds compared to the total contract price of approximately £2m. Despite the light weight the roof has been found to be very stable during recent high velocity and gusting wind conditions.

4. Calgary Exhibition and Stampede Grandstand, Canada (Project)

Figure 10 shows a cross section of the grandstand structure. Figure 9 shows a photograph of a model of the complete project.

In this case a design study has been carried out and model tests undertaken to determine the effect of damping in varying configurations. The basic design of a grandstand precludes any attachments to the forward portion of the roof and consequently in this instance the only practical place to apply damping was along the line of the roof directly above the rear row of seats in the grandstand. These dampers would be positioned to act both in the vertical plane and also angled at 45° to the vertical such that damping would be achieved vertically and on any horizontal movement of the roof perpendicular to the line of the seating (indicated on Figure 10).

A fibreglass model of the roof was constructed and subjected to constant force vibration on a moving coil vibrator and various damping arrangements were tested. From the model tests carried out it is possible to determine the size and form of damping system to be installed in the full scale project (Figure 11).

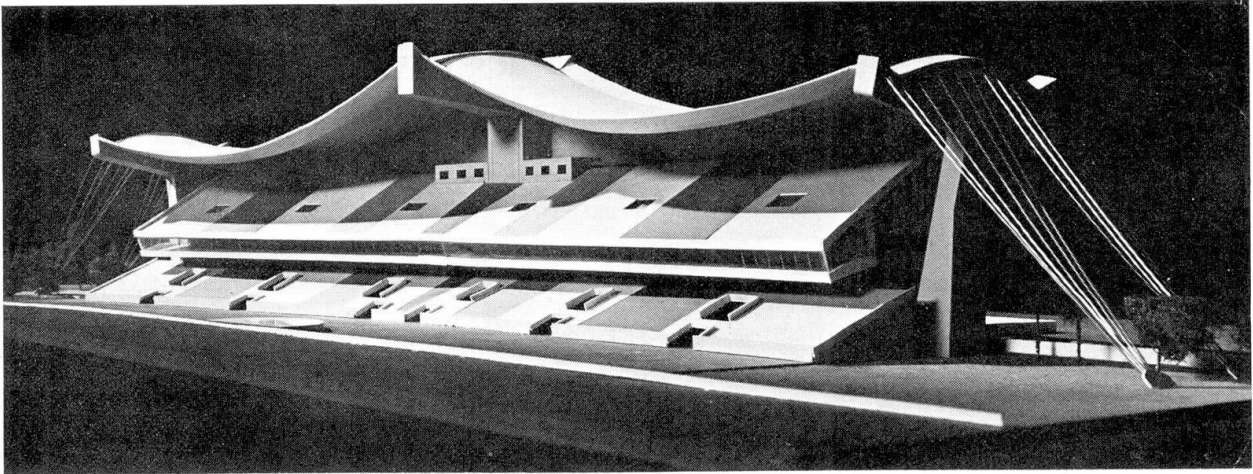


Figure 9.

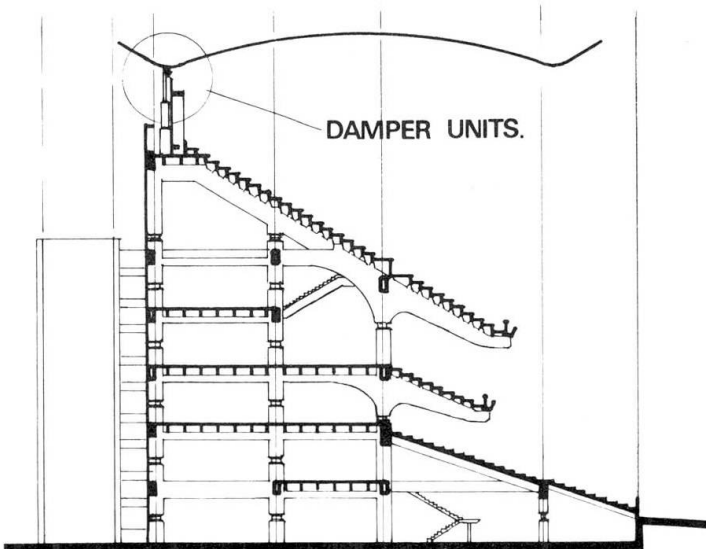


Figure 10.

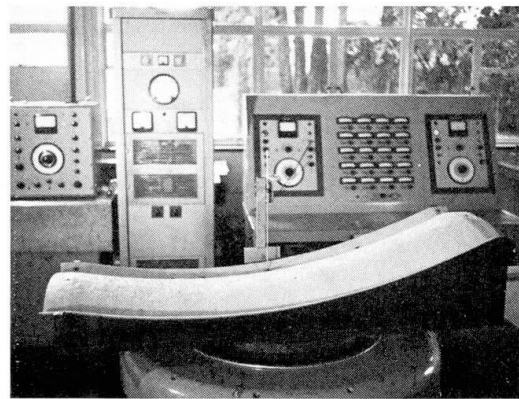


Figure 11.

The cost of testing together with that of the damping system was assessed to be under \$100,000 whereas increasing the weight and stiffness of the roof to be safe without dampers could have easily reached or even exceeded \$1m.

This particular structural solution was not finally proceeded with, as due to strict budget limitations a saving had to be made. This was achieved by moving the whole grandstand back from the arena, decreasing the number of seats at the top balcony and adding them at ground level. The width of the roof, covering seats, was reduced from 33.5 m to 20 m enabling adoption of cantilever solution within the budget limitations.

5. The advantages of lightweight damped roofs

In the paper by Abeles² under Theme V, it has been pointed out that certain stiffness is required for structures subjected to wind vibration to ensure that the amplitude is not too high and the natural frequency differs from that of vortex shedding frequency at characteristic wind velocity. With the addition of suitable dampers these limitations can be overcome and light modern roofs can be constructed safely and economically. This was achieved in all three examples by the combination of structural design and added damping at low cost.

The weights of the three roofs are 244 kg/m^2 , 165 kg/m^2 and 220 kg/m^2 respectively. These compare very favourably with a weight of 650 kg/m^2 at which according to K. Yokota³ of the Aoki Research Centre, Tokyo, rigidity of a structure was obtained for the roof of the famous Myoden temple of the Sho Hondu complex, Japan.

References

1. T. Maciag "The Prestressed Lightweight Concrete Roof for Doncaster Race-Course Grandstand", paper presented at the Sixth International Congress of the Fédération Internationale de la Précontrainte, Prague, June 1970.
2. P.W. Abeles "The Resistance of Prestressed Concrete to Dynamic Loading, Its Fatigue Resistance; Miner's Hypothesis", Theme V.
3. K. Yokota "Rigid Members Frame 22,000 ton Hung Roof", Engineering News Record, August 17 1972.

SUMMARY

It has been shown that the combination of lightweight design with added damping can result in the construction of roofs giving satisfactory performance at a total cost a fraction of that of the rigid high density design. It has also been demonstrated how the damping devices can be incorporated into the design without imposing limits on the structural or architectural aspects.

RESUME

On montre dans ce travail que la combinaison de structures de couverture légères et de systèmes d'amortissement permet de construire des toits au comportement satisfaisant et d'un coût total inférieur à celui des structures courantes rigides plus lourdes. On explique aussi comment le mécanisme amortisseur peut être intégré à la structure sans imposer des limites à l'aspect structural ou à l'aspect architectural.

ZUSAMMENFASSUNG

Es wurde gezeigt, dass die Kombination der Leichtbauweise mit eingebauter Dämpfung in modernen Dachkonstruktionen mit befriedigendem Verhalten die Gesamtkosten auf einen Bruchteil senken kann, verglichen mit der Ausführung mit den üblichen Baustoffen. Ebenso wurde gezeigt, wie die Dämpfungsvorrichtungen in den Entwurf mit einbezogen werden können, ohne den baulichen und architektonischen Aspekten Grenzen zu setzen.